

## Paper 11

# EFFECT OF BY-PASS CHARACTERISTICS ON PARALLEL-CHANNEL FLOW INSTABILITIES

By M. B. Carver\*

Experiments on parallel-channel hydrodynamic stability frequently use one heated channel operating in parallel with an unheated by-pass. This arrangement is designed to simulate the operation of a particular channel in a boiling water reactor; the by-pass providing the essentially constant pressure drop which the remaining channels impose on the channel in question.

If the ratio of by-pass flow to channel flow is large the changes in channel flow do not significantly affect the overall pressure drop; however, particularly in experiments using full-scale reactor fuel channels, loop capacity may limit this by-pass ratio. In this case the pressure drop is no longer constant.

This paper shows, analytically, that a low by-pass ratio, resulting in a variable overall pressure drop, significantly affects the dynamic behaviour of the heated channel. Both the power at threshold of flow oscillation and the natural frequency of the system are shown to depend on by-pass characteristics. In particular, a heated channel operating with a low by-pass ratio is normally stable to much higher powers than it is with a high by-pass ratio.

A linearized analysis is presented which illustrates the effect of by-pass resistance and inertia on the threshold power and natural frequency of flow oscillations. The analysis is incorporated in a computer code, and resulting threshold powers and oscillation frequencies are compared to data from experiments using a full-scale simulated reactor channel in parallel with a by-pass.

It is concluded that the finite unheated by-pass does not accurately simulate the dynamic effect of the remaining reactor channels on a particular channel. However, the methods of this paper should prove useful in interpreting results from a flow-limited test loop and extrapolating to the full reactor case.

## INTRODUCTION

THE PHENOMENON of parallel-channel flow instability is of particular concern to designers of boiling water reactors. In such reactors, the coolant normally passes through the reactor core in numerous parallel tubes, which operate between common reservoirs. The fuel is inserted in the coolant tubes, often forming a complex cross-sectional flow geometry.

It is well known that flow instability may be prevented by providing a substantial inlet throttling on the individual coolant channels. Economic incentives, however, demand a more accurate determination of the minimum adequate inlet throttling.

The analytical approach to this problem has been to consider a 'hot channel'. This is a channel which has a

combination of high power and low inlet throttling, making it the most prone to instability. The effect of any disturbance in flow in this channel is assumed to be distributed amongst the many remaining channels. As all channels operate between common reservoirs, and the flow changes in all other channels are small, a constant pressure drop is imposed across the hot channel. Although in many reactors there may be a small group of hot channels, the same approach applies, and the philosophy of the method is still basically sound.

In approaching the problem experimentally, however, it is not feasible to set up a large number of parallel heated channels. A common approach has been to set up a single heated test section operating in parallel with a large unheated by-pass. If the by-pass ratio, which is defined as the ratio of by-pass flow to test section flow, is very large, fluctuations in test section flow do not significantly affect by-pass flow and again the pressure drop remains essentially constant.

*The MS. of this paper was received at the Institution on 2nd April 1969 and accepted for publication on 23rd May 1969. 22*

\* *Research Engineer, Atomic Energy of Canada Limited, Chalk River, Ontario, Canada.*

To simulate a reactor channel adequately in such an experiment, a simulated reactor channel test section must be used, and high mass fluxes are required. Many experimental loops do not have the capacity to provide sufficient by-pass ratio to keep the pressure drop constant. The problem which then arises is: 'What effect, if any, does the by-pass ratio have on the dynamic behaviour of the heated channel?'

This paper presents an analysis of the effect of the by-pass on the stability of flow in the heated channel in the experimental configuration described above. The equations of the analysis have been incorporated in a computer programme. Stability boundaries and oscillation frequencies from the computer programme are compared with results from experiments using a full-scale simulated reactor channel operating in parallel with a by-pass.

### Notation

$A$	Cross-sectional area, ft <sup>2</sup> .
$B$	Flow dependent function.
$E$	Flow dependent function.
$F$	Friction and restriction loss coefficient.
$f$	Friction factor.
$G$	Mass flux, lb/ft <sup>2</sup> s.
$g$	Acceleration due to gravity, ft/s <sup>2</sup> .
$H_z$	Enthalpy distribution function.
$\Delta H$	Total enthalpy rise, Btu/lb.
$h$	Specific enthalpy, Btu/lb.
$I$	Inertia ( $I = L/gA$ ).
$J$	Constant defined by $J = 1/gA^2$ .
$K$	Restriction loss coefficient.
$L$	Length, ft.
$P$	Pressure, lb/ft <sup>2</sup> .
$\Delta P$	Pressure drop, lb/ft <sup>2</sup> .
$Q$	Heat input, Btu/s.
$q$	Heat flux, Btu/ft s.
$\bar{q}$	Average heat flux, Btu/ft s.
$R_z$	Density distribution function.
$s$	The Laplace variable.
$t$	Time, s.
$W$	Mass flow, lb/s.
$z$	Axial co-ordinate, ft.
$\gamma$	By-pass ratio.
$\xi$	Damping factor.
$\rho$	Density, lb/ft <sup>3</sup> .
$\omega$	Frequency, 1/s.

$a, b, c, d, e, \alpha, \beta, \theta, \Psi$  are characteristic equation coefficients and are defined in text.

### Subscripts

$b$	By-pass.
$c$	Channel.
$f$	Frictional and restrictional.
$n$	At resonance.
$z$	Axial distribution.
$\infty$	At constant pressure drop.

Numerical subscripts refer to positions in Fig. 11.1, except when applied to distinguish coefficients in the transfer function [equation (11.20)].

### ANALYSIS

Fig. 11.1 shows the geometry of the system under consideration. Single-phase flow  $W_0$  enters the system at A and may pass either to the heated test section or the unheated by-pass. The two flow streams recombine at D. Flows may be controlled by adjusting any of the four valves.

To simplify the analysis, the following assumptions are made:

- (1) The total system flow,  $W_0$ , is constant.
- (2) The inlet temperature and pressure are constant.
- (3) The by-pass stream is adiabatic.

The one-dimensional conservation equations for the system may now be written.

### Formulation and linearization of the equations

#### Equations for the channel

Energy:

$$W_c \frac{\partial h_c}{\partial z} + \rho_c A_c \frac{\partial h_c}{\partial t} = q \quad (11.1)$$

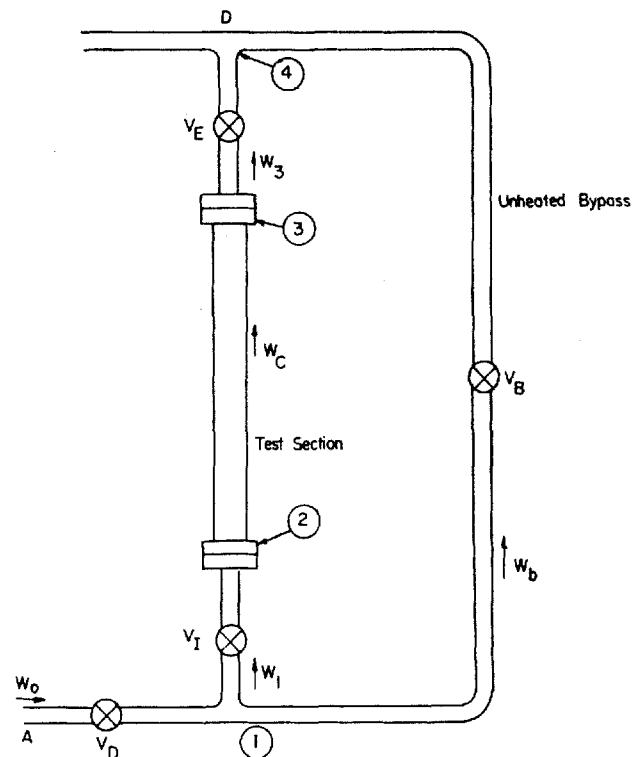


Fig. 11.1. Unheated by-pass operating in parallel with two-phase test section

Continuity:

$$\frac{\partial W_c}{\partial z} + A_c \frac{\partial \rho_c}{\partial t} = 0 \quad \dots \quad (11.2)$$

Momentum:

$$-\frac{\partial P_{23}}{\partial z} = \frac{f_c}{2gD_c A_c^2} \cdot \frac{W_c^2}{\rho_c} + \frac{1}{gA_c^2} \cdot \frac{\partial}{\partial z} \left( \frac{W_c^2}{\rho_c} \right) + \frac{1}{gA_c} \cdot \frac{\partial W_c}{\partial t} + \frac{K_c}{2gA_c^2} \cdot \frac{W_c^2}{\rho_c} + \rho_c \quad (11.3)$$

State:

$$\rho = f(h) \quad \dots \quad (11.4)$$

Equations for the by-pass

$$-\frac{\partial P_{14}}{\partial z} = \frac{f_b}{2gD_b A_b^2} \cdot \frac{W_b^2}{\rho_b} + \frac{K_b}{2gA_b^2} \cdot \frac{W_b^2}{\rho_b} + \frac{1}{gA_b} \cdot \frac{dW_b}{dt} + \rho_b \quad \dots \quad (11.5)$$

$$\Delta P_{14} = \Delta P_{12} + \Delta P_{23} + \Delta P_{34} \quad \dots \quad (11.6)$$

$$W_b + W_1 = W_0 = \text{const.} \quad \dots \quad (11.7)$$

Equations for the inlet and outlet feeders

$$-\Delta P_{12} = \frac{fL_1}{2gD_1 A_1^2} \cdot \frac{W_1^2}{\rho_1} + \frac{K_1}{2gA_1^2} \cdot \frac{W_1^2}{\rho_1} + \rho_1 z_1 + \frac{L_1}{gA_1} \cdot \frac{dW_1}{dt} \quad \dots \quad (11.8)$$

$$-\Delta P_{34} = \frac{fL_3}{2gD_3 A_3^2} \cdot \frac{W_3^2}{\rho_3} + \frac{K_3}{2gA_3^2} \cdot \frac{W_3^2}{\rho_3} + \rho_3 z_3 + \frac{L_3}{gA_3} \cdot \frac{dW_3}{dt} \quad \dots \quad (11.9)$$

where  $W_3$  and  $\rho_3$  are average values in the outlet pipe.

These equations may now be simplified by combining frictional and restriction loss terms and writing:

$$\frac{f_i L_i}{g_i D_i A_i^2} + \frac{K_i}{g A_i^2} = F_i, \quad \frac{L_i}{g A_i} = I_i, \quad \frac{1}{g A_i^2} = J_i \quad \dots \quad (11.10)$$

and dropping the subscript  $c$ .

Employing these modifications and linearizing, equations (11.1)–(11.9) become:

$$W \frac{\partial \Delta h}{\partial z} + \frac{\partial h}{\partial z} \Delta W + \rho A \frac{\partial \Delta h}{\partial t} = \Delta q \quad (11.11)$$

$$\frac{\partial \Delta W}{\partial z} + A \frac{\partial \Delta \rho}{\partial t} = 0 \quad \dots \quad (11.12)$$

$$-\frac{\partial \Delta P_{23}}{\partial z} = \frac{F_c W}{\rho} \Delta W - \frac{F_c W^2}{2\rho^2} \Delta \rho + \Delta \rho + J_c \frac{\partial}{\partial z} \left[ \frac{2W}{\rho} \Delta W - \frac{W^2}{\rho^2} \Delta \rho \right] + \frac{I}{L} \cdot \frac{\partial \Delta W}{\partial t} \quad (11.13)$$

$$\Delta \rho = \frac{\partial \rho}{\partial h} \Delta h \quad \dots \quad (11.14)$$

$$\Delta(\Delta P_{14}) = \frac{F_b W_b}{\rho_1} \Delta W_b + I_b \frac{\partial \Delta W_b}{\partial t} \quad (11.15)$$

$$\Delta(\Delta P_{12}) = \frac{F_1 W_1}{\rho_1} \Delta W_1 + I_1 \frac{\partial \Delta W_1}{\partial t} \quad (11.16)$$

$$\Delta(\Delta P_{34}) = \frac{F_3 W_3}{\rho_3} \Delta W_3 + I_3 \frac{\partial \Delta W_3}{\partial t} + \Delta \rho_3 z_3 - \frac{F_3 W_3^2}{2\rho_3^2} \Delta \rho_3 \quad \dots \quad (11.17)$$

$$\Delta(\Delta P_{12}) + \Delta(\Delta P_{23}) + \Delta(\Delta P_{34}) = \Delta(\Delta P_{14}) \quad (11.18)$$

$$\Delta W_b + \Delta W_1 = 0 \quad \dots \quad (11.19)$$

In an earlier publication, Quandt (1)\* presented an analysis of a heated channel operating at constant pressure drop. By assuming a linear axial distribution of flow, Quandt developed an expression relating the inlet and outlet flows  $\Delta W_1$  and  $\Delta W_3$  to pressure drop,  $\Delta(\Delta P_{14})$ . For the constant pressure drop case [ $\Delta(\Delta P_{14}) = 0$ ] the transfer function  $\Delta W_1 / \Delta W_3$  follows immediately. Quandt's analysis yields the following equations, which are developed in Appendix 11.1:

$$\Delta(\Delta P_{14}) = \Delta W_1 \left( a_1 + b_1 s + \frac{c_1}{s} \right) + \Delta W_3 \left( a_2 + b_2 s + \frac{c_2}{s} \right) \quad \dots \quad (11.20)$$

$$\Delta W_3 = \frac{d_1/s + e_1}{d_2/s + e_2} \Delta W_1 + \frac{\Delta Q}{d_2/s + e_2} \quad (11.21)$$

In order to include the by-pass, equations (11.15), (11.18), and (11.19) are now transformed and combined:

$$\begin{aligned} \Delta(\Delta P_{14}) &= \frac{F_b W_b}{\rho_1} \Delta W_b + I_b s \Delta W_b \\ &= -\frac{F_b W_b}{\rho_1} \Delta W_1 - I_b s \Delta W_1 \quad (11.22) \end{aligned}$$

Inserting equation (11.21) into equation (11.20),

$$0 = \Delta W_1 \left[ \left( a_1 + \frac{F_b W_b}{\rho_1} \right) + (b_1 + I_b) s + \frac{c_1}{s} \right] + \Delta W_3 \left[ a_2 + b_2 s + \frac{c_2}{s} \right]$$

or

$$\frac{\Delta W_3}{\Delta W_1} = -\frac{[(\beta_1) s^2 + (\alpha_1) s + c_1]}{[b_2 s^2 + a_2 s + c_2]} \quad (11.23)$$

Equations (11.21) and (11.23) are now combined to eliminate  $\Delta W_3$ :

$$\frac{d_1/s + e_1}{d_2/s + e_2} + \frac{\Delta Q}{\Delta W_1} \cdot \frac{1}{d_2/s + e_2} = -\frac{\beta_1 s^2 + \alpha_1 s + c_1}{b_2 s^2 + a_2 s + c_2} \quad (11.24)$$

Noting that  $d_1 = d_2$  and  $c_2 = -c_1$ , this may be simplified to give:

$$\frac{\Delta W_1}{\Delta Q} = -\frac{b_2 s^2 + a_2 s + c_1}{s^2(e_1 b_2 + \beta_1 e_2) + s[d_1(b_2 + \beta_1) + e_1 a_2 + e_2 \alpha_1] + (a_2 + \alpha_1) d_1 + e_1(e_2 - e_1)} \quad \dots \quad (11.25)$$

### Stability

The stability is governed by the damping term, i.e. the coefficient of  $s$  in the denominator:

$$\xi = d_1(b_2 + \beta_1) + e_1 a_2 + e_2 \alpha_1$$

\* References are given in Appendix 11.2.

If this term is zero, oscillations will be generated by a small flux perturbation. Expanding the term (see Appendix 11.1) and rearranging gives:

$$\xi = \frac{W_c}{R} (I_1 + I_c + I_3 + I_b) - \Delta H \left[ \frac{F_3 W_3}{\rho_3} - \int_0^L \frac{\partial}{\partial W} \cdot \frac{\partial P_f}{\partial z} \left(1 - \frac{z}{L}\right) dz \right] + \left( H_2 + \frac{R_z}{R} \right) \left[ \frac{F_1 W_1}{\rho_1} + \frac{F_3 W_3}{\rho_3} + \frac{F_b W_b}{\rho_1} - 2 \int_0^L \frac{\partial}{\partial W} \cdot \frac{\partial P_f}{\partial z} \left(1 - \frac{z}{L}\right) dz \right] \quad (11.26)$$

Examining this it may be seen immediately that the following terms, involving by-pass characteristics, increase  $\xi$  and are stabilizing:

- (1) By-pass inertia  $I_b$ .
- (2) By-pass friction and restriction loss,

$$\frac{F_b W_b}{\rho_1} = \frac{\gamma F_b W_1}{\rho_1}$$

Note that this involves both by-pass ratio,  $\gamma$ , and loss coefficient,  $F_b$ , but these are in fact related.

For steady state one can equate flow-dependent pressure drops:

$$F_b W_b^2 = F'_c W_1^2$$

where  $F'_c$  includes channel and feeders, i.e.

$$F_b \gamma^2 W_1^2 = F'_c W_1^2, \text{ or } \gamma^2 F_b = F'_c$$

That is, for given channel conditions, by-pass ratio can only be changed by changing  $F_b$ , the by-pass control valve. Thus

$$\frac{\partial}{\partial F_b} \left( \frac{F_b W_b}{\rho_1} \right) = \frac{W_1 \sqrt{F'_c}}{\rho_1} \cdot \frac{\partial}{\partial F_b} (F_b)^{1/2} = + \frac{W_1}{2\rho_1} \sqrt{\frac{F'_c}{F_b}}$$

Therefore, an increase in the by-pass resistance stabilizes the system, and it is destabilized by an increase in the by-pass ratio.

On inspection of equation (11.26) the normal conclusions regarding the effect of channel and feeder variables on stability are also apparent [see reference (1)].

### Frequency

The effect of by-pass ratio on frequency may also be determined by examining the remaining terms of the characteristic equation.

Coefficient of  $s^2$ :

$$\theta = e_1 b_2 + \beta_1 e_2 = (I_1 + I_c + I_3 + I_b) \left( H_2 + \frac{R_z}{R} \right) - \Delta H \left( I_3 + \frac{I_c}{2} \right)$$

Constant term:

$$\Psi = (a_2 + \alpha_1) \alpha_1 + c_1 (e_2 - e_1) = \left( \Gamma_{1c} + \frac{F_b W_b}{\rho_1} \right) \frac{W_c}{R} + C \Delta H$$

where  $C$  and  $\Gamma_{1c}$  represent terms not involving by-pass parameters.

Thus

$$\omega_n^2 = \Psi / \theta = \left[ \frac{\left( \Gamma_{1c} + \frac{F_b W_b}{\rho_1} \right) \frac{W_c}{R} + C \Delta H}{\left( H_2 + \frac{R_z}{R} \right) (\sum I_c + I_b) - \Delta H \left( I_3 + \frac{I_c}{2} \right)} \right] \quad (11.27)$$

$$\frac{\partial(\omega_n^2)}{\partial F_b} = \text{const.} \frac{\partial}{\partial F_b} \left( \frac{F_b W_b}{\rho_1} \right) > 0, \quad \frac{\partial(\omega_n^2)}{\partial I_b} < 0$$

That is, frequency increases with increased by-pass resistance, or decreased by-pass ratio, and decreases with increased by-pass inertia.

The above explains qualitatively the effect of by-pass parameters on stability. To obtain a quantitative assessment, the non-linear equations [equations (11.1)-(11.9)] have been included in an existing computer code which solves them using finite difference methods.

### THE COMPUTER CODE

The computer code, POISE, has been described in earlier publications (2) (3). The code solves the non-linear conservation equations by using finite differences in time and space in equations (11.1)-(11.4), (11.8), and (11.9). The method of integration is that developed by Tong *et al.* (4). The solution for the rate of change of channel inlet mass flux yields

$$\frac{dG_1}{dt} = E(G) \Delta P + B(G) \quad (11.28)$$

where  $\Delta P$  is the constant header to header pressure drop, and  $E$  and  $B$  are functions containing time and flow dependent pressure drops. For the present analysis  $\Delta P$  is no longer constant but depends on channel and by-pass flows. Equations (11.5)-(11.7) may be incorporated into equation (11.28) by the method given below.

Integrate equation (11.5), incorporating equation (11.10):

$$\Delta P_{14} = \frac{F_b W_b^2}{\rho_1} + I_b \frac{dW_b}{dt} + \rho_1 Z_b \quad (11.29)$$

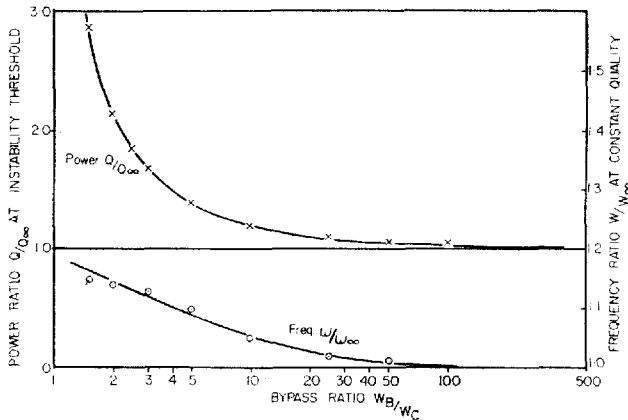
Substitute for  $W_b$  from equation (11.7), noting  $W_1 = A_c G_1$

$$\Delta P_{14} = \frac{F_b (W_0 - A_c G_1)^2}{\rho_1} - I_b A_c \frac{dG_1}{dt} + \rho_1 Z_b \quad (11.30)$$

Equations (11.30) and (11.28) are now combined to give

$$\frac{dG_1}{dt} = \frac{E(G) \left( \frac{F_b (W_0 - A_c G_1)^2}{\rho_1} \right) + \rho_1 Z_b + B(G)}{1 + I_b A_c} \quad (11.31)$$

To confirm the qualitative conclusions drawn from the linear analysis, the POISE code was modified to include equation (11.31) and appropriate supporting equations. Powers and oscillation frequencies at the stability boundary for a given set of initial conditions (channel flow, pressure, inlet temperature, and feeder resistances) were obtained over a range of by-pass ratios. The results, shown in Fig. 11.2, confirm the relationships suggested by the linearized



Subscript  $\infty$  refers to infinite by-pass ratio.

Fig. 11.2. Effect of by-pass ratio on threshold of stability and frequency for a typical set of flow conditions

analysis. It can be seen that the stability boundary power becomes very large at zero by-pass ratio. This is consistent with standard critical heat flux tests which are done without by-pass and normally exhibit no significant flow oscillations.

**COMPARISON TO EXPERIMENTAL RESULTS**

The results from the computer code have been compared to the experiments of Collins and Gacesa (5). As the experiments are described fully in references (5) and (6), only a brief description is given here.

**Experimental loop**

The experiments were done on the SWIFT loop at Canadian Westinghouse Company. The loop delivers subcooled water to a test section-by-pass combination similar to that shown in Fig. 11.1. The test section was geometrically similar to a 19-rod bundle reactor coolant channel with the fuel rods simulated by electrical heaters. Geometrical details are given in Table 11.1. Test section and by-pass flows and upstream heater temperatures were recorded continuously.

**Experimental results**

For all experiments the required test section flow, inlet temperature, pressure, and feeder valve positions were set

Table 11.1. SWIFT test section dimensions

Shroud:	
Inside diameter, in . . . . .	3.936
Bundle:	
Element diameter, in . . . . .	0.75
Heated length, in . . . . .	196.8
Heated perimeter, in . . . . .	44.76
Cross-sectional area, in <sup>2</sup> . . . . .	8.4
Number of elements . . . . .	19
Flow area, in <sup>2</sup> . . . . .	3.567
Wetted perimeter, in . . . . .	56.13
Equivalent diameter, in . . . . .	0.254

initially. Power was then increased by increments until stable or periodic dry-out occurred on one or more of the heaters. The total flow was held constant, and the mean by-pass and test section flows were maintained constant throughout the test by adjusting the by-pass valve. Two significant powers were associated with each flow oscillation: the threshold of periodic dry-out (TPD) was defined as the lowest power at which resonant flow oscillations were sufficiently severe to make dry-out occur periodically at the low flow portion of the cycle; the threshold of flow oscillation (TFO) was defined as the power at which oscillations at the resonant frequency were first observed in the flow trace. The former is easily distinguished from the flow trace but detection of the latter is more subjective.

**Basis for comparison**

The computer code gives the stability boundary; that is, the power at which a further perturbation generates a continuously diverging oscillation. This is normally analogous to the experimental TPD, because if a diverging oscillation is permitted to persist in an experiment the minimum flow eventually becomes low enough for periodic dry-out to occur. In certain tests a small amplitude, non-diverging oscillation was sufficient to produce periodic dry-out. The TPD power in such cases is obviously below the stability threshold, but as all tests were terminated at TPD this power is the best available estimate of threshold power.

**Comparison of results**

The power at stability boundary from the computer code is compared to experimental TPD powers from reference (5) in Table 11.2, and Figs 11.3–11.6. As the computer programme has been compared extensively to earlier experimental results (2) (3), only those experiments which indicated the variation of TPD power with by-pass ratio, other conditions being equal, have been selected for comparison.

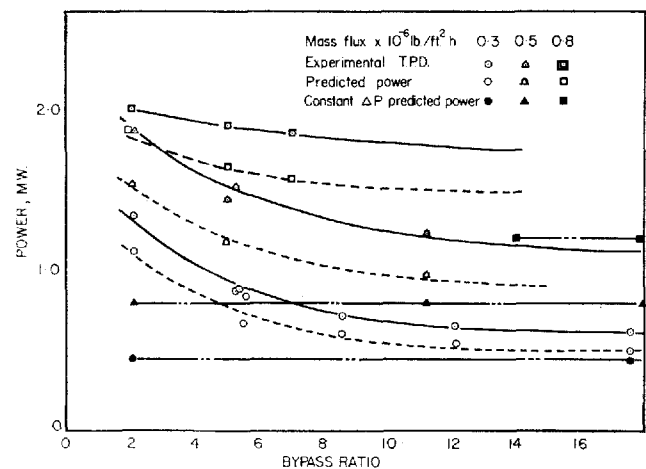


Fig. 11.3. Comparison of experimental and predicted values of power at stability threshold

Table 11.2. Comparison of POISE predictions to selected tests

Test	Nominal experimental initial conditions					Experimental TPD results			Computer code predictions					
	Mass flux $\times 10^{-6}$ , lb/ft <sup>2</sup> h	Exit sub- cooling, °F	Exit pressure, lb/in <sup>2</sup> (abs.)	Feeder loss coefficients		By-pass ratio	Q Power, MW	X Quality, %	$\tau$ Period, s	With by-pass ratio			Constant $\Delta p$	
				In	Out					Q Power, MW	X Quality, %	$\tau$ Period, s	Q Power, MW	X Quality, %
140	0.3	30	800	320	220	5.3	0.88	56	6.7	0.68	36	4.3	0.45	19
141						8.6	0.73	44	7.2	0.60	32	4.4		
143						5.4	0.90	54	6.9	0.68	36	4.3		
145						2.1	1.35	87	8.0	1.12	66	4.0		
146						5.6	0.85	50	6.7	0.68	36	4.3		
148						12.1	0.64	39	6.8	0.55	30	4.5		
149						17.6	0.61	41	6.5	0.50	27	4.5		
150	0.5	30	800	160	150	11.2	1.25	45	4.7	1.00	33	3.0	0.76	22
153						5.0	1.43	53	4.2	1.20	39	2.9		
154						2.1	1.86	65	3.8	1.90	52	2.8		
156						5.4	1.54	56	3.5	1.25	43	3.0		
165	0.75	30	800	37	65	5.0	1.92	40	3.0	1.70	33	2.5	1.20	21
169						6.9	1.82	38	2.9	1.58	29	2.6		
170						2.0	2.02	46	3.0	1.90	38	2.5		
171	0.75	30	800	37	65	0		Stable		Stable				
181	1.0	37	800	14	40	5.0	1.80	29	2.9	1.65	26	1.9	1.24	17
182						3.0	2.13	35	3.0	2.02	32	1.8		
184						7.0	1.53	26	3.6	1.83	28	1.9		
186						7.0	1.40	24	3.5	1.50	24	2.0		
192						5.5	1.58	26	3.0	1.59	25	1.9		
195						5.5	1.90	31	3.0	1.93	30	1.8		

In Fig. 11.3, computed stability thresholds are compared to experimental TPD powers at nominal mass velocities of  $0.3$ ,  $0.5$ , and  $0.8 \times 10^6$  lb/ft<sup>2</sup> h. In all cases the computed stability threshold is lower than experimental power, and the variation of power with by-pass ratio is the same. For comparison, the stability threshold computed at constant pressure drop is also shown.

In Fig. 11.4, computed and experimental powers are compared at  $1 \times 10^6$  lb/ft<sup>2</sup> h mass velocity for two values of outlet restriction. The computed values are not as sensitive to outlet restriction as the experimental results in this case.

Fig. 11.5 is an attempt to isolate the effect of by-pass ratio. For each of the experimental curves in Figs 11.3 and 11.4, power has been normalized by dividing by experi-

mental power at a by-pass ratio of 5. The computed curves have been normalized using the computed power at a by-pass ratio of 5. All power ratios thus obtained have been plotted against the reciprocal of by-pass ratio. The reciprocal has been used to permit inclusion of the computed infinite by-pass ratio points. Experimental and computed points show good agreement in the effect of by-pass ratio.

A comparison is made in Fig. 11.6 of the power at incipience of oscillation (experimental TFO) and the computed stability threshold. Again the effect of by-pass ratio is apparent, but the difficulty in consistently extracting the TFO power from the flow trace has caused some scatter of the experimental results.

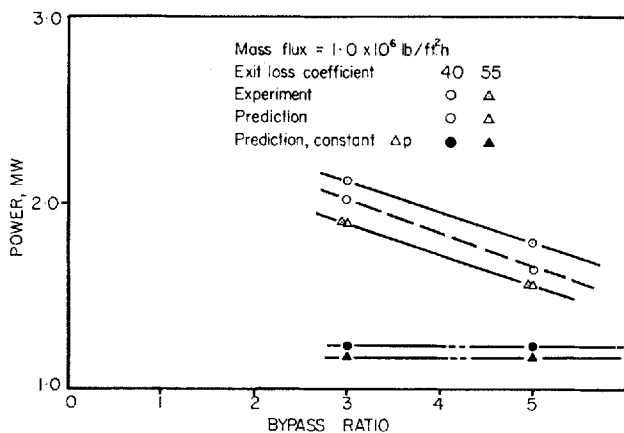


Fig. 11.4. Comparison of experimental and predicted stability threshold powers at two values of exit throttling

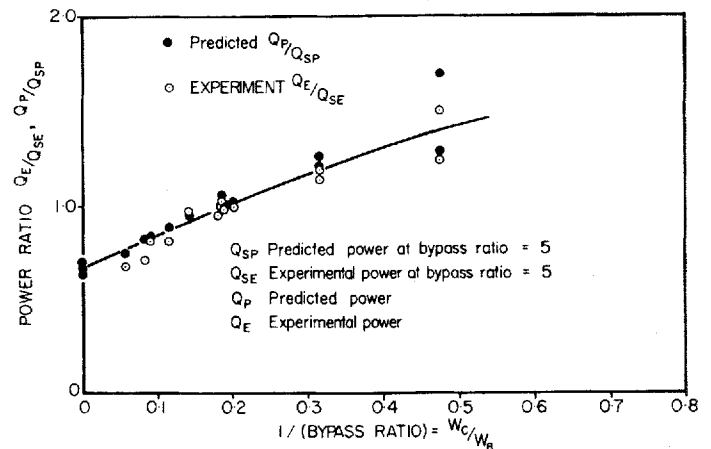


Fig. 11.5. Effect of by-pass ratio on stability threshold power (all tests)

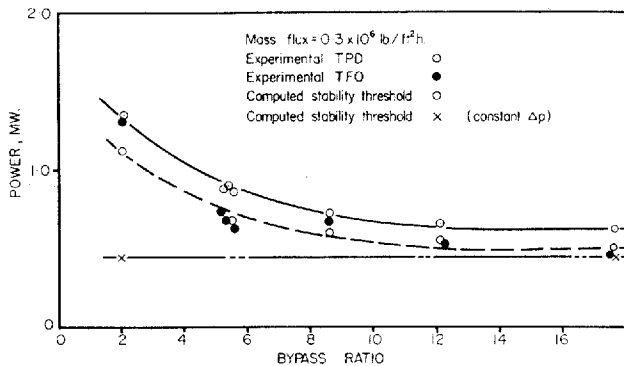


Fig. 11.6. Comparison of computed stability threshold power to experimental TPD and TFO powers

### DISCUSSION

Both experiment and analysis show that the stability boundary is strongly affected by the by-pass characteristics. An examination of equation (11.26) shows that stability depends specifically on by-pass inertia and loss factor. The experimental programme so far has investigated only the effect of changing by-pass ratio by varying the by-pass control valve. By-pass ratio may also be varied at constant flow by controlling either feeder valve. It is therefore important to recognize by-pass ratio as a dependent variable; the individual loss coefficients in the feeders and by-pass are independent variables.

This concept proves useful in explaining apparent anomalies in previous experiments. Before the by-pass equations were incorporated, the POISE programme was used in comparison with similar experiments at Columbia University (7). The constant pressure drop programme showed a far greater variation of stability with outlet feeder throttling than was shown by the experiments (8). As these experiments were also conducted at quite low by-pass ratios, an increase in outlet throttling at constant total flow would tend to reduce the flow, and additional by-pass throttling is therefore required to maintain channel flow and by-pass ratio. The destabilizing effect of the exit throttle has been partially offset by the increase in by-pass resistance. In the constant pressure drop case there is, of course, no such reaction and the outlet throttle consequently has greater effect.

The present comparisons show that the computer code always provides a conservative estimate of the power at which diverging oscillations occur, while the power at which incipient oscillations first appear is roughly comparable to computed power. At large by-pass ratios both the limiting value of TFO power and the computed power approach the stability boundary computed for constant pressure drop, while the TPD power converges to a higher asymptote.

The code computes an oscillation frequency consistently higher than the experimental value. Examination of Table 11.2 shows the ratio of experimental to computed frequency to be about 0.65. The same relationship was

noted in comparison with the Columbia University experiments. However, when the programme was compared to experiments using annuli and tubes, much better agreement in frequency was obtained (3). The model can deal only with a channel of specified area, wetted perimeter, and heated perimeter, and this is probably sufficient for a simple cross-section geometry. However, in the multi-rod bundles used in the Columbia and SWIFT experiments, exchange of flow between the various inter-connected flow passages may significantly affect oscillation frequencies.

It was not possible to extract sufficient information on the variation of frequency with by-pass ratio from the experiments. Fig. 11.2 shows that the computed variation of frequency with by-pass ratio is a small effect compared to the variation of power, and experimental results show considerable scatter.

### THE PARALLEL HEATED CHANNEL CASE

Calculations using the POISE code show that if two or more heated channels are used in parallel, instead of a single heated channel with an unheated by-pass, the stability power does not strongly depend on the number of channels. The two-channel case is the most stable, but the ratio of threshold power with two channels to the constant pressure drop power is below 1.2.

This is supported by the good agreement observed when the constant pressure drop version of the code was compared to experiments in a rig using three parallel channels (3).

### CONCLUSIONS

The finite unheated by-pass does not accurately simulate the dynamic effect of the remaining heated channels on a particular reactor coolant channel, because overall pressure drop is not independent of channel disturbances at low by-pass ratio.

The relationship of stability threshold with by-pass resistance is of an exponential form. Stability threshold power approaches the constant pressure drop value at high by-pass ratios and becomes very high at zero by-pass ratio.

A computer programme originally used to predict stability threshold at constant pressure drop has been modified to include the effect of by-pass characteristics and the results agree well with experimental evidence.

Experiments using a finite by-pass in parallel with a heated test section may now be extrapolated to the multi-heated channel, constant pressure drop reactor case by using a computed relationship between by-pass ratio and stability threshold.

### ACKNOWLEDGEMENTS

The author is indebted to D. B. Collins and W. T. Hancox of Canadian Westinghouse Co. Ltd, and W. B. Nicoll of the University of Waterloo, who have all been frequently involved in discussions of this subject.

APPENDIX 11.1

DEVELOPMENT OF THE RELATIONSHIP BETWEEN INLET FLOW, OUTLET FLOW, AND PRESSURE DROP This section closely follows the method of reference (1) and is therefore described only briefly.

The equations are simplified by assuming a linear axial flow relationship, and a flux weighted axial enthalpy distribution.

Let

$$\Delta W = \Delta W_1 + (\Delta W_3 - \Delta W_1) \frac{z}{L} \quad (11.32)$$

$$\Delta h = \Delta h_3 \frac{z'}{L} \quad (11.33)$$

where

$$\frac{z'}{L} = \frac{1}{L} \int_0^L \frac{q(z, t)}{\bar{q}(t)} dz \quad (11.34)$$

This allows for the effect of heat flux distribution on enthalpy profile.

These may now be inserted into equations (11.11)–(11.19). Substituting equations (11.20) and (11.21) into equation (11.12) and integrating gives:

$$\Delta W_3 - \Delta W_1 = - \left[ \frac{\partial \Delta h_3}{\partial t} A \int \frac{\partial \rho}{\partial h} \frac{z'}{L} dz \right] = R \frac{\partial \Delta h_3}{\partial t} \quad (11.35)$$

where  $R$  is a function of heat flux distribution and steady-state conditions.

Equation (11.11) may also be expanded and integrated:

$$W \Delta h_3 + \Delta W_1 \Delta \bar{H} + (\Delta W_3 - \Delta W_1) \int_0^L \frac{\partial h}{\partial z} \frac{z}{L} dz + A \frac{\partial \Delta h_3}{\partial t} \int_0^L \rho \frac{z'}{L} dz = \int_0^L \Delta q dz \quad (11.36)$$

Equations (11.35) and (11.36) are now transformed and combined to give:

$$\Delta h_3 = \frac{1}{R_s} (\Delta W_3 - \Delta W_1)$$

$$W \Delta h_3 + \Delta W_1 \Delta \bar{H} + (\Delta W_3 - \Delta W_1) H_z + s \Delta h_3 R_z = \Delta Q$$

where

$$\Delta \bar{H} = \text{total enthalpy rise,}$$

$$H_z = \int_0^L \frac{\partial h}{\partial z} \frac{z}{L} dz, \quad R_z = A \int_0^L \rho \frac{z'}{L} dz$$

Rearranging:

$$\Delta W_3 = \frac{\left( \frac{W}{R_s} + H_z + \frac{R_z}{R} - \Delta \bar{H} \right)}{\left( \frac{W}{R_s} + H_z + \frac{R_z}{R} \right)} \Delta W_1 + \frac{\Delta Q}{\left( \frac{W}{R_s} + H_z + \frac{R_z}{R} \right)} \quad (11.37)$$

This relates outlet flow to inlet flow and heat input.

The momentum equation [equation (11.13)] may now be transformed and integrated along the channel:

$$\begin{aligned} \Delta(\Delta P_{23}) &= F_c W \int_0^L \frac{\Delta W}{\rho} dz - \frac{F_c W^2}{2} \int \frac{\Delta \rho}{\rho^2} dz + \int_0^L \Delta \rho dz \\ &+ J_c \left[ \left( \frac{2W}{\rho} \Delta W - \frac{W^2}{\rho^2} \Delta \rho \right) \right]_0^L + \frac{I_c}{L_c} s \int_0^L \Delta W dz \end{aligned} \quad (11.38)$$

Combining equation (11.26) with the transformed versions of equations (11.16)–(11.18), and collecting terms, gives:

$$\begin{aligned} \Delta(\Delta P_{14}) &= \Delta W_1 \left[ \left( \frac{F_1 W_1}{\rho_1} - \frac{2WJ_c}{\rho_1} \right) + I_1 s \right] \\ &+ \Delta W_3 \left[ \frac{2WJ_c}{\rho_3} + \frac{F_3 W_3}{\rho_3} + I_3 s \right] \\ &+ \Delta \rho_3 \left[ \frac{W^2 J_c}{\rho_3^2} - \frac{F_3 W_3^2}{\rho_3^2} + z_3 \right] - \frac{F_c W^2}{2} \int_0^L \frac{\Delta P}{\rho} dz \\ &+ F_c W \int_0^L \frac{\Delta W}{\rho} dz + \int_0^L \Delta \rho dz + \frac{I_c}{L} s \int_0^L \Delta W dz \end{aligned} \quad (11.39)$$

Now, combine equations (11.14), (11.33), and (11.35):

$$\Delta \rho = \frac{\partial \rho}{\partial h} \Delta h = \frac{\partial \rho}{\partial h} \Delta h_3 \frac{z'}{L} = \frac{\partial \rho}{\partial h} \frac{z'}{L} \frac{\Delta W_3 - \Delta W_1}{R_s} \quad (11.40)$$

and use equation (11.32):

$$\int_0^L \Delta W dz = (\Delta W_3 + \Delta W_1) \frac{L}{2} \quad (11.41)$$

Also note that as  $\partial P_f / \partial z = F_c (W^2 / 2\rho)$ ,

$$\frac{\partial}{\partial W} \left( \frac{\partial P_f}{\partial z} \right) = \frac{F_c W}{\rho} \quad \text{and} \quad \frac{\partial}{\partial \rho} \left( \frac{\partial P_f}{\partial z} \right) = - \frac{F_c W^2}{2\rho^2} \quad (11.42)$$

Substituting equations (11.40)–(11.42) into equation (11.39) gives  $\Delta(\Delta P_{14})$  in terms of  $\Delta W_1$  and  $\Delta W_3$ :

$$\begin{aligned} \Delta(\Delta P_{14}) &= \Delta W_1 \left[ \left( \frac{F_1 W_1}{\rho_1} - \frac{2WJ_c}{\rho_1} - \int_0^L \frac{\partial}{\partial W} \left( \frac{\partial P_f}{\partial z} \right) \right. \right. \\ &\quad \times \left( 1 - \frac{z}{L} \right) dz \left. \right) + \left( I_1 + \frac{I_c}{2} \right) s \\ &\quad + \frac{1}{R_s} \left( \int_0^L \frac{\partial}{\partial \rho} \left( \frac{\partial P_f}{\partial z} \right) \frac{\partial \rho}{\partial h} \frac{z'}{L} dz \right. \\ &\quad \left. - \int_0^L \frac{\partial \rho}{\partial h} \frac{z'}{L} dz \right. \\ &\quad \left. - \left( \frac{\partial \rho}{\partial h} \right)_3 \left( \frac{W^2 J_c}{\rho_3^2} - \frac{F_3 W_3^2}{\rho_3^2} + z_3 \right) \right] \\ &+ \Delta W_3 \left[ \left( \frac{F_3 W_3}{\rho_3} + \frac{2WJ_c}{\rho_3} - \int_0^L \frac{\partial}{\partial W} \left( \frac{\partial P_f}{\partial z} \right) \frac{\partial P_f}{\partial z} \left( \frac{z}{L} \right) dz \right) \right. \\ &\quad \left. + \left( I_3 + \frac{I_c}{2} \right) s \right. \\ &\quad \left. - \frac{1}{R_s} \left( \int_0^L \frac{\partial}{\partial \rho} \left( \frac{\partial P_f}{\partial z} \right) \frac{\partial \rho}{\partial h} \frac{z'}{L} dz \right) \right. \\ &\quad \left. - \int_0^L \frac{\partial \rho}{\partial h} \frac{z'}{L} dz \right. \\ &\quad \left. - \left( \frac{\partial \rho}{\partial h} \right)_3 \frac{z'}{L} \left( \frac{W^2 J_c}{\rho_3^2} - \frac{F_3 W_3^2}{\rho_3^2} + z_3 \right) \right] \end{aligned} \quad (11.43)$$

For simplification, this may be written:

$$\Delta(\Delta P_{14}) = \Delta W_1 \left( a_1 + b_1 s + \frac{c_1}{s} \right) + \Delta W_3 \left( a_2 + b_2 s + \frac{c_2}{s} \right) \quad (11.44)$$

and equation (11.37) may also be simplified:

$$\Delta W_3 = \frac{d_1/s + e_1}{d_2/s + e_2} \Delta W_1 + \frac{\Delta Q}{d_2/s + e_2} \quad (11.45)$$

The definitions of  $a$ ,  $b$ ,  $c$ , etc. may be found by referring to equations (11.43) and (11.37).

## APPENDIX 11.2

### REFERENCES

- (1) QUANDT, E. R. 'Analysis and measurement of flow oscillations', *Chem. Eng. Progress*, Monograph and Symposium Series No. 32-5, *Heat Transfer, Buffalo, N.Y.*, 111.
- (2) CARVER, M. B. 'An analytical model for the prediction of hydrodynamic instability in parallel heated channels', *Rept No. AECL-2681* 1967 (March) (Atomic Energy of Canada Limited).
- (3) CARVER, M. B. 'The influence of certain design variables on the hydrodynamic stability of a heated channel', A.S.M.E. Paper 67-HT-66; *Rept No. AECL-2976* (Atomic Energy of Canada Limited).
- (4) TONG, L. S. *Boiling heat transfer and two-phase flow* 1965, 209 (Wiley, New York).
- (5) COLLINS, D. B. and GACESA, M. 'Hydrodynamic instability experiments in a full-scale simulated reactor channel with an unheated by-pass', paper to be submitted to the Symposium on Fluid Mechanics and Measurement in Two-Phase Flow Systems, Leeds University 1969 (September).
- (6) HANCOX, W. T. and NICOLL, W. B. 'Flow oscillation in a channel heated by 19-rod bundles with an unheated by-pass—comparison of analytical predictions with experimental data', CWAPD-120 1969 (January) (to be published).
- (7) MATZNER, B., CASTERLINE, J. E. and KOKOLIS, S. 'Critical heat flux and flow stability in a 9 ft 19-rod test section simulating a string of short discrete rod bundles', *Topical Rept 10*, Task XVI of Contract AT(30-3)-187, Columbia University, N.Y., 1968 (June).
- (8) CARVER, M. B., D'ARCY, D. F., WIKHAMMER, G. A., CASTERLINE, J. E. and MATZNER, B. 'Instabilities in flow through multi-rod bundles and their effect on dryout', Paper D-4, *Symp. Research in Cocurrent Gas-Liquid Flow, University of Waterloo* 1968 (September); *Rept No. AECL-2716* (Atomic Energy of Canada Limited).